(6) Scott, R. L. *J. Chem. Phys.* **1949**, *17*, 279.
(7) Morra, B. S.; Stein, R. S. *J. Polym. Sci., Polym. Phys. Ed.* **1982**, *20*, 2243.
(8) Rim, P. B.; Runt, J. P. *Macromolecules* **1983**, *16*, 762.
(9) Hoffman, J. D.; Weeks, J. J. *J. Chem. Phys.* **1962**, *37*, 1723.
(10) Hoffman, J. D.; Weeks, J. J. *J. Res. Natl. Bur. Stand., Sect. A* **1962**, *66*, 13.
(11) Eshuis, A.; Roerdink, E.; Challa, G. *Polymer* **1982**, *23*, 735.
(12) Calahorra, E.; Cortazar, M.; Guzmán, G. M. *Polymer* **1982**, *23*, 1322.
(13) Martuscelli, E.; Silvestre, C.; Gismondi, C. *Makromol. Chem.* **1985**, *186*, 2161.
(14) Martuscelli, E.; Pracella, M.; Yue, W. P. *Polymer* **1984**, *25*, 1097.
(15) Plans, J.; MacKnight, W. J.; Karasz, F. E. *Macromolecules* **1984**, *17*, 810.
(16) Woo, E. M.; Barlow, J. W.; Paul, D. R. *Polymer* **1985**, *26*, 763.
(17) Jonza, J. M.; Porter, R. S. *Macromolecules* **1986**, *19*, 1946.
(18) Katime, I. A.; Anasagasti, M. S.; Peleteiro, M. C.; Valenciano, R. *Eur. Polym. J.* **1987**, *23*, 907.
(19) Briber, R. M.; Khoury, F. *Polymer* **1987**, *28*, 38.
(20) Min, K. E.; Chiou, J. S.; Barlow, J. W.; Paul, D. R. *Polymer* **1987**, *28*, 1721.
(21) Zhang, H.; Prud'homme, R. E. *J. Polym. Sci., Part B: Polym. Phys.* **1987**, *25*, 723.
(22) Howsmon, J. A.; Marchessault, R. H. *J. Appl. Polym. Sci.* **1959**, *1*, 313.
(23) Tadokoro, H.; Kozai, K.; Seki, S.; Nitta, I. *Kobunshi Kangaku* **1959**, *16*, 418.
(24) Paul, D. R.; Barlow, J. W.; Bernstein, R. E.; Wahrmund, D. C. *Polym. Eng. Sci.* **1978**, *18*, 1225.
(25) Ziska, J. J.; Barlow, J. W.; Paul, D. R. *Polymer* **1981**, *22*, 918.
(26) Kwei, T. K.; Patterson, G. D.; Wang T. T. *Macromolecules* **1976**, *9*, 780.
(27) Harris, J. E.; Goh, S. H.; Paul, D. R.; Barlow, J. W. *J. Appl. Polym. Sci.* **1982**, *27*, 839.

Communications to the Editor

Study of the $T(1)$ Transition of Poly[bis(trifluoroethoxy)phosphazene] Using Solid-State Nuclear Magnetic Resonance Spectroscopy

Considerable interest has been developed in thermotropic polymers generally over the past decade or more.[1-3] In semicrystalline polyphosphazenes three transitions have been established: glass temperature T_g, thermotropic (mesophase) transition $T(1)$, and melting transition, T_m. Whenever the side-group chemistry is altered, these parameters scale linearly[4] in a plot of $(T_m - T_g)/(T_m - T(1)$ against $T(1)/T_m$. The first-order transitions $T(1)$ and T_m are well-known for poly[bis(trifluoroethoxy)phosphazene] (PBFP),[3] typically $T(1) \sim 85$ °C and $T_m \sim 242$ °C. T_g lies well below these transitions at approximately −66 °C. Interestingly, there is a significant change in the location and magnitude of the $T(1)$ transition whenever polyphosphazenes are heated and cooled. In PBFP specifically crystallized from solution, samples are usually spherulitic. Small-angle X-ray measurements made on crystal mats formed at room temperature indicate that lamellae of ~140 Å are obtained. The crystallinity of these specimens is suprisingly low (<50%) and the crystal structure is monoclinic. When heated through $T(1)$ the sample undergoes some form of chain extension. The thermotropic state is comprised of molecules hexagonally packed in arrays or domains. In this condition they have considerable fluidity as creep and other measurements substantiate.[5] The interchain spacing has been assessed by X-ray and electron diffraction,[6] which confirms the hexagonal arrangement in the 2D δ-state.[6,7] Whenever PBFP is cooled from the molten state it returns very rapidly to the 2D hexagonally packed phase and finally crystallizes into a 3D orthorhombic structure below $T(1)$ (i.e., different from the original monoclinic form). [After the first thermal cycle through $T(1)$, the 3D orthorhombic phase dominates below $T(1)$.] Apparently the transformation occurs through relatively small displacements or translations in the chain direction so as to allow growth to occur laterally with an Avrami[8] $n = 2$. The crystallinity of PBFP returned to room temperature is much higher than the starting specimen and the location and enthalpy of the $T(1)$ transition is increased substantially upon thermal cycling. The chain packing and the resultant 3D ordering shows that $T(1)$ and $\Delta H[T(1)]$ asymptotically approach an upper limit in PBFP and in other polyphosphazenes.[3] Dilatometry measurements[5] clearly indicate the first-order nature of $T(1)$ and T_m as well as a significant volume change (~6%) that is associated with material expansion and enhanced mobility that occurs at both of these temperatures.

Wide-line nuclear magnetic resonance (NMR) and X-ray measurements were made on PBFP about a decade ago.[9] It was reported that the thermotropic state of this polymer is involved with rapidly rotating chains in a hexagonal lattice that exhibited both lateral order and longitudinal disorder. This condition or state was attributed to the onset of rapid side group and backbone chain motions.

Now that solid-state NMR has emerged as a technique for studying local molecular dynamics and conformational changes through decoupling side group and main-chain motions, its application to polyphosphazenes is not surprising. The first high-resolution solid-state NMR study of polyphosphazenes was reported only 1 year ago by Crosby and Haw.[10] ^{31}P magic-angle spinning (MAS) NMR was used to examine the hydrolysis and cross-linking of poly(dichlorophosphazene). The molecular dynamics of poly(dimethyloxyphosphazene) (PBMP) and poly(diethoxyphosphazene) (PBEP) was studied by ^{31}P MAS and ^{13}C cross-polarization (CP)/MAS NMR at various temperatures. The results from this investigation indicate that the main chains of PBEP and PBMP are undergoing large-amplitude anisotropic motions above their respective glass transition temperatures. Crosby and Haw concluded that ^{31}P MAS and ^{13}C CP/MAS NMR can be used to study molecular dynamics in phosphazene polymers.

More recently Tonelli and co-workers[11,12] investigated the phase transitions of poly[bis(*p*-ethylphenoxy)phosphazene] (PBEPP). They used ^{31}P MAS/dipolar decoupling (DD) at several temperatures and found a sudden decrease in line width corresponding to the crystal–liquid crystal transition which occurred above 100 °C. They concluded that considerable backbone motion occurs whenever PBEPP passes into the thermotropic phase. From the spin–lattice relaxation times, T_1 of the carbon atoms on the side group, they reported that the side chains were also mobile in the thermotropic phase. According to this work, short spin–lattice relaxation times observed only for the protonated aromatic carbons in the 3D crystal indicate that phenyl rings are mobile and rotating about their 1,4-axes even below the $T(1)$ transition.

0024-9297/89/2222-2549$01.50/0

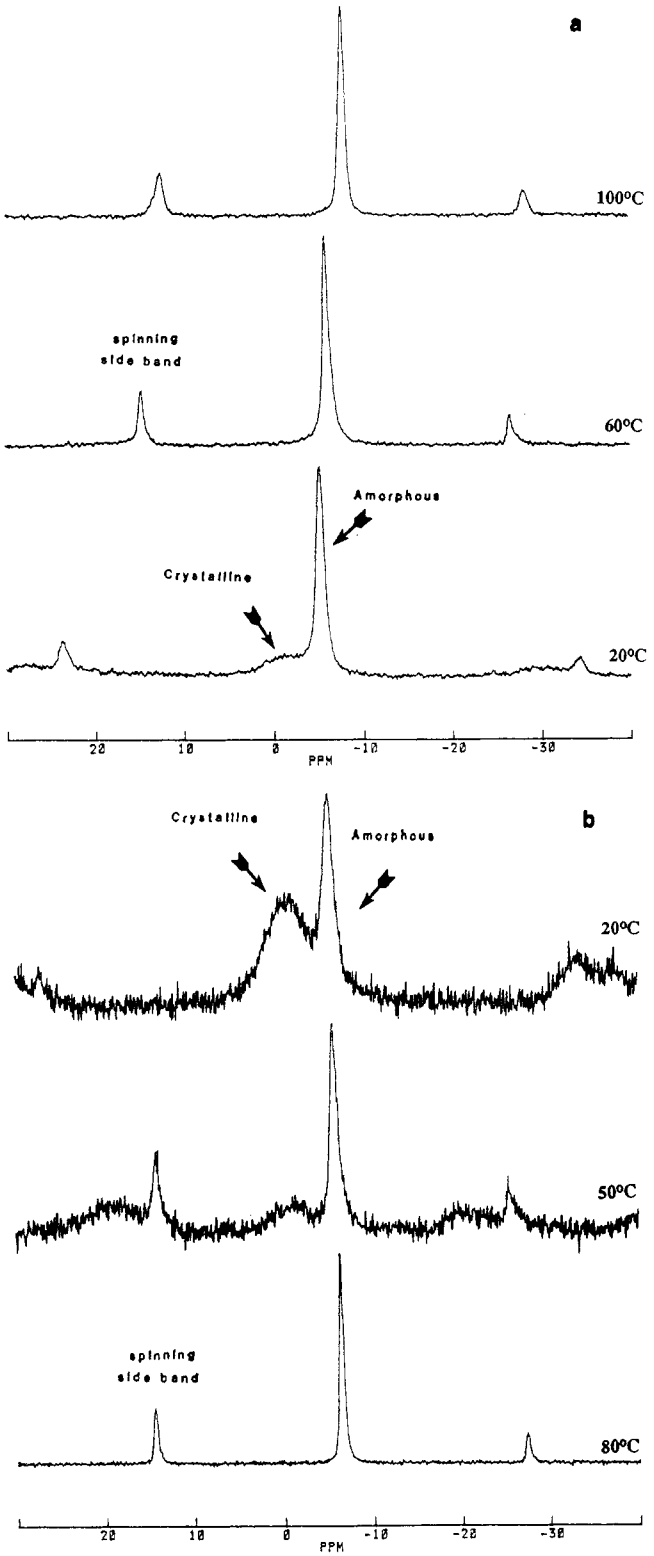

Figure 1. (a) ^{31}P NMR spectra of PBFP at 20, 60, and 100 °C during heating. (b) ^{31}P NMR spectra of PBFP at 80, 50, and 20 °C during cooling from 100 °C.

Experimental Section. Solution-crystallized poly[bis(trifluoroethoxy)phosphazene] (PBFP) (M_w = 300 000 and M_w/M_n = 2.3) was studied in our laboratory by ^{31}P and ^{13}C MAS variable-temperature NMR. ^{1}H decoupling was used for ^{13}C but not for ^{31}P. The spectra were recorded between room temperature and 100 °C on a Brüker MSL 300 NMR spectrmeter. Magic angle sample spinning was performed at speeds of 2.0–4.0 kHz. The samples were spun in aluminum oxide rotors with Teflon end caps. ^{31}P

Table I
Percent Crystallinity of PBFP Assessed from Relative Areas of the Amorphous and Crystalline ^{31}P Peaks

temp, °C	crystallinity	amorphous
1st heating		
20	25%	75%
30	25%	75%
40	16%	84%
50	9%	91%
1st cooling		
50	35%	65%
40	48%	52%
30	50%	50%
20	54%	46%
2nd heating		
30	52%	48%
40	41%	59%
50	14%	86%
2nd cooling		
60	23%	77%
40	35%	65%
24	54%	46%

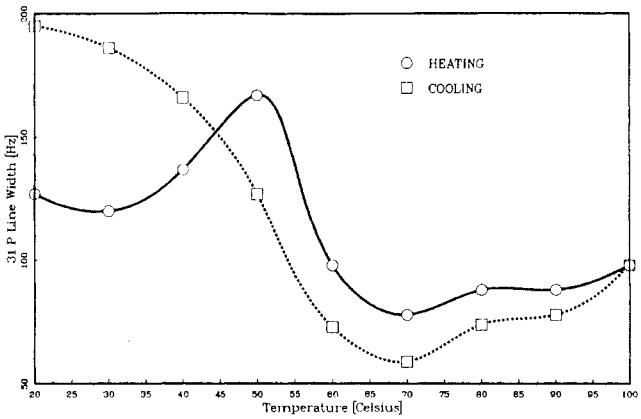

Figure 2. ^{31}P MAS line width from the amorphous phase of PBFP during heating and cooling (first thermal cycle).

spectra were recorded at 10 °C intervals from 20 to 100 °C, which was the upper limit of this equipment. The sample was then cooled at 10 °C intervals and spectra were recorded at each interval. This procedure was repeated to ensure reproducibility.

Figure 1a shows selected ^{31}P NMR spectra for PBFP obtained during the heating process at 20, 60, and 100 °C and Figure 1b provides spectra recorded during the cooling process at 80, 50, and 20 °C. Below the $T(1)$ transition there are two peaks corresponding to the amorphous and crystalline regions. (Amorphous in this context is presumed to be a structure that has less than 3D order.) As the polymer is heated through $T(1)$ and cooled down again to room temperature, the peak area corresponding to the crystalline region increases, in accordance with DSC and X-ray measurements. The relative areas of the crystalline and amorphous peaks are listed in Table I as a function of thermal history.

The ^{31}P chemical shift referenced against H_3PO_4 (0 ppm) of the amorphous phase decreases as the temperature increases. A small increase in the ^{31}P chemical shift occurs just before the $T(1)$ transition temperature is reached, corresponding to a change in conformation as the chain backbone extends. This change is affected by the coexisting crystalline phase. The decrease in magnitude of the chemical shift suggests that the nuclei are becoming more shielded as the temperature is increased during the transformation into the 2D thermotropic phase. The magnitude of the chemical shift increases with thermal cycling as the state of the material alters.

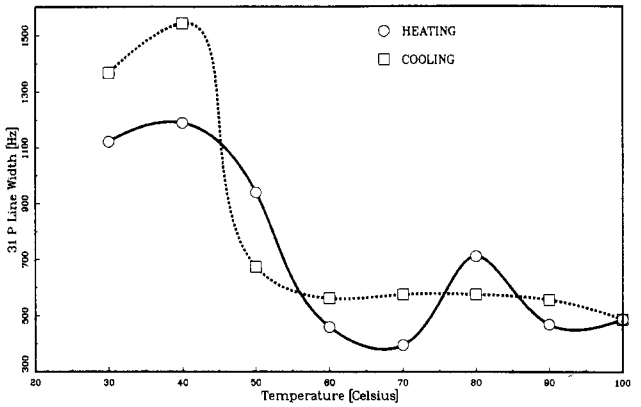

Figure 3. ^{31}P MAS line width of PBFP during heating and cooling after annealing at 200 °C.

The temperature dependence of the ^{31}P line width of the amorphous phase during the first heating cycle is shown in Figure 2. Note that the line width sharpens as more thermal energy enters the sample, except at temperatures just before the $T(1)$ transition. The increase in the line width which occurs just before $T(1)$ is reached is probably due to reorganization taking place before this transition. Cooling after the heating cycle results in an increase in the spectral line width that is measured at room temperature. During the second heating the spectral line width drops to a minimum value before peaking at approximately 75 °C, as compared to 50 °C that is observed for the first heating cycle. An enhancement of 3D ordering occurs upon cycling the sample as the results in Table I indicate.

^{13}C MAS ^{1}H-decoupled NMR spectra of PBFP obtained at 23 and 100 °C were almost identical except for a small decrease in line width of the single peak, which is consistent with the enhanced mobility of the CH_2 portion of the side group in $[—N=P(OCH_2CF_3)_2—]_x$. As the sample passes through the $T(1)$ transition it occupies a larger volume according to dilatometry results made on PBFP.[5] It therefore follows that the side chains have mobility even in the 3D phase of PBFP. The fluorine atoms on the end carbon atom split the signal into a quartet as anticipated from their chemical structure. Furthermore, ^{13}C spin–lattice relaxation measurements made through $T(1)$ for the CH_2 and CF_3 side groups on PBFP are 1.7 and 3.5 s, respectively. The corresponding activation energies associated with these groups are estimated to be $E_{CH_2} \sim 17.3$ kJ/mol and $E_{CF_3} \sim 13.7$ kJ/mol.

Since the upper temperature limit for in situ spinning in our Brüker spectrometer was limited to 100 °C, the PBFP sample was annealed at 200 °C outside of the instrument and slowly cooled to room temperature again. The ^{31}P MAS NMR plot of line width versus temperature of this sample is shown in Figure 3. The spectral line width measured at room temperature is now much broader than it was before annealing. However, as the specimen temperature is increased stepwise in 10 °C intervals to 100 °C, the line width sharpens. This behavior is more pronounced (three to four times), but it is still consistent with the trend found before annealing. The increased line width observed at 30 °C is due to the inherently higher crystallinity, which now suppresses the mobility of the phosphorus–nitrogen backbone below $T(1)$. These results are in accord with the observations of Sun and Magill,[3] who found that annealing and thermal cycling of PBFP and other polyphosphazenes also increases their crystallinity. Solution ^{31}P NMR was performed on the PBFP sample to determine if the chemical structure was altered due to annealing. A sharp singlet at −6.9 ppm before and after annealing indicated that no chemical change had occurred.

In conclusion, these preliminary results serve to show that solid-state variable-temperature NMR is a useful technique that can be used to study in situ molecular chain dynamics, chain conformation, and specimen crystallinity, in accordance with the morphology of PBFP. Two distinct crystalline and amorphous regions are clearly exhibited by the chain backbone below $T(1)$. A single highly mobile ordered 2D phase exists above $T(1)$, in line with our other solid-state observations and properties. The $-OCH_2CF_3$ side branches of the polymer exhibit mobility below the $T(1)$ transition and appear to have a similar mobility and conformation on either side of the $T(1)$ transition. The crystalline–amorphous ratio in PBFP assessed by solid-state NMR is strongly dependent upon annealing conditions and temperature of measurement.

Acknowledgment. We thank Professor George Marcelin for use of the NMR facilities, Dr. F. T. Lin for performing the solution NMR, and the National Science Foundation (Polymers Program, DMR 8509412) and the Office of Naval Research (Chemistry Division, N0001485K0358) for support of the work.

References and Notes

(1) Singler, R. E.; Schneider, N. S.; Hagnauer, G. L. *Polym. Eng. Sci.*, **1975**, *15*, 321.
(2) Alcock, H. R. *Sci. Prog.* **1980**, *66*, 355.
(3) Sun, D. C.; Magill, J. H. *Polymer* **1987**, *28*, 1243.
(4) Kojima, M.; Magill, J. H. In *Morphology of Polymers*; Sedlacek, B., Ed.; Walter de Gruyter & Co.; New York, 1986.
(5) Masuko, M.; Simeone, R. L.; Magill, J. H.; Plazek, D. J. *Macromolecules* **1984**, *17*, 2857.
(6) Kojima, M.; Magill, J. H. *Makromol. Chem.* **1985**, *186*, 649.
(7) Schneider, N. S.; Desper, C. R. In *Liquid Crystalline Order*; Blumstein, A., Ed.; Academic Press: New York, 1978; Chapter 9.
(8) Ciora, R. J.; Sun, D. C.; Magill, J. H. *Proceedings Sixteenth North American Thermal Analysis Society*; Washington, DC, Sept 27–30, 1987; p 325.
(9) Alexander, M. N.; Desper, C. R.; Sagalyn, P. L.; Schneider, N. S. *Macromolecules* **1977**, *10*, 721.
(10) Crosby, R. C.; Haw, J. F. *Macromolecules* **1987**, *20*, 2324.
(11) Tonelli, A. E.; Gomez, M. A.; Tanaka, H.; Schilling, F. C. *Polymer Prepr.* **1988**, *29*, 440.
(12) Tanaka, H.; Gomez, M. A.; Tonelli, A. E.; Chichester-Hicks, S. V.; Haddon, R. C. *Macromolecules* **1988**, *21*, 2301.

† Also Materials Science and Engineering Department.

Scott G. Young and Joseph H. Magill*,†
School of Engineering, University of Pittsburgh
Pittsburgh, Pennsylvania 15261

Received December 14, 1988;
Revised Manuscript Received March 6, 1989

Polyethylene Crystallinity from Static, Solid-State NMR Spectra

It is well-known that linear polyethylene (LPE) rapidly crystallizes from the melt to form a semicrystalline solid with an amorphous phase and a crystalline phase. The interactions between these phases and the relative proportion of each phase are important factors affecting the bulk properties of the material.[1] A great deal of effort has been expended to accurately determine the crystallinity in semicrystalline polymers; the most common methods are X-ray diffraction, density measurement, differential scanning calorimetry (DSC), and ^{1}H broad line NMR. High-resolution, cross-polarized, magic angle spinning (CP/MAS) ^{13}C NMR can distinguish the crystalline phase

